Supplementary Information for:

Representing methane emissions from wet tropical forest soils using microbial functional groups constrained by soil diffusivity

Debjani Sihi[1], Xiaofeng Xu[2], Mónica Salazar Ortiz[3], Christine S. O'Connell[4,5], Whendee L. Silver[5], Carla López-Lloreda[6], Julia M. Brenner[1], Ryan K. Quinn[1,7], Jana R. Phillips[1], Brent D. Newman[8], and Melanie A. Mayes[1]*

[1]Climate Change Science Institute and Environmental Sciences Division, Oak Ridge National Laboratory, Oak Ridge, TN, 37831, USA
[2]Department of Biology, San Diego State University, San Diego, CA, 92182-4614, USA
[3]Institute of Plant Science and Microbiology, University of Hamburg, Hamburg, 20148, Germany
[4]Department of Environmental Studies, Macalester College, St. Paul, MN, 55105-1899, USA
[5]Department of Environmental Science, Policy and Management, University of California, Berkeley, CA, 94720-3114, USA
[6]Department of Natural Resources and the Environment, University of New Hampshire, Durham, NH, 03824, USA
[7]Department of Biology, Boston University, Boston, MA, 02215, USA
[8]Earth and Environmental Sciences Division, Los Alamos National Laboratory, Los Alamos, NM, 87545, USA

Correspondence to: Melanie A. Mayes (mayesma@ornl.gov)

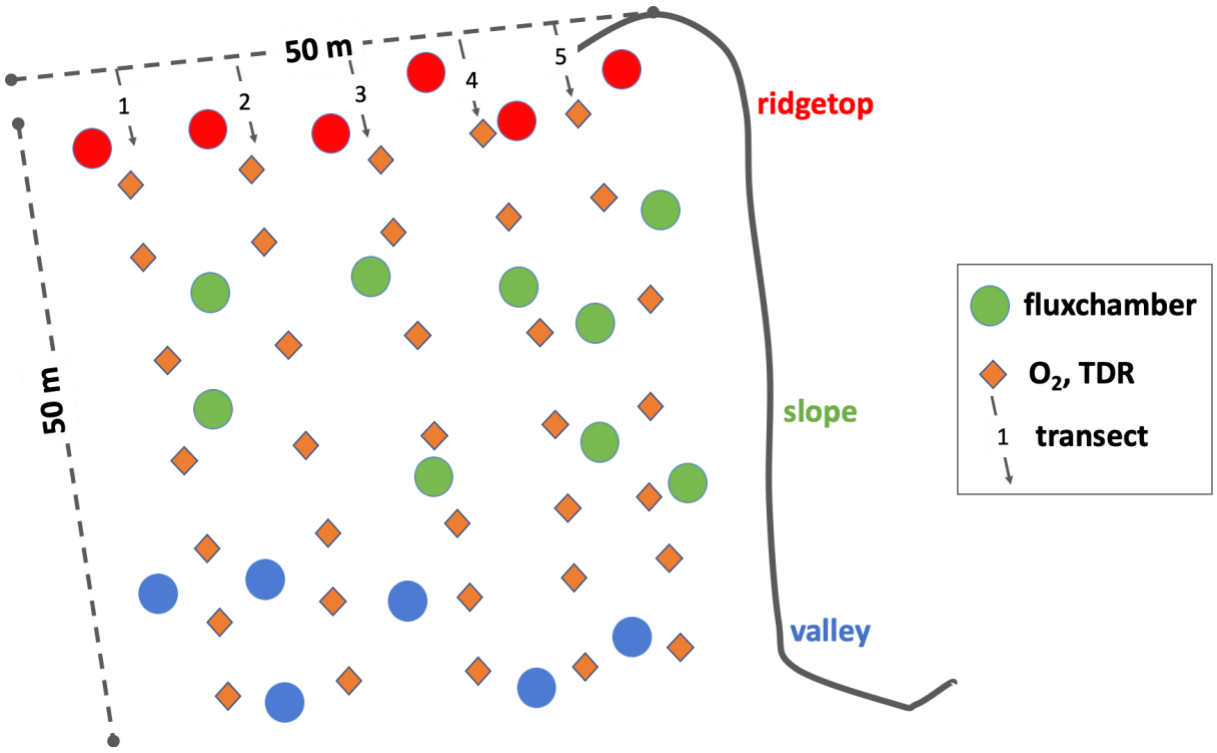

Figure S1: Array of fluxchambers and sensor transects 1-5 for oxygen (O_2) and temperature and soil moisture (TDR) across the catena in Luquillo Experimental Forest in Puerto Rico (figure modified from O'Connell et al. (2018)).

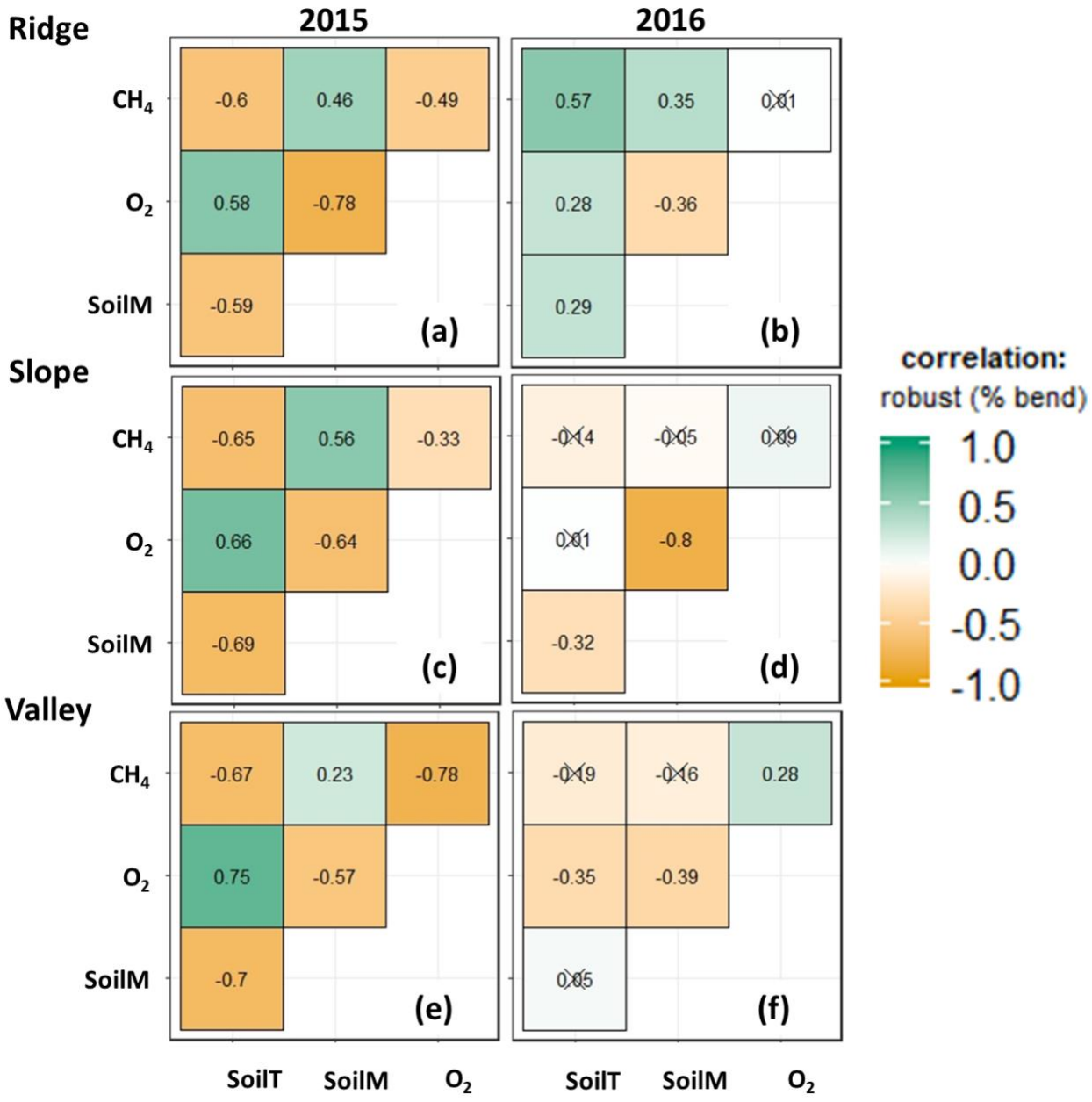

Figure S2: Relation between soil meteorology and methane emissions for 2015 (a, c, e) and 2016 (b, d, f). SoilM, SoilT, O_2, CH_4 represent soil moisture, soil temperature, oxygen, and methane, respectively. Numbers represent adjusted Holm correlation coefficients, and numbers with "X" indicate a non-significant correlation at $p < 0.05$.

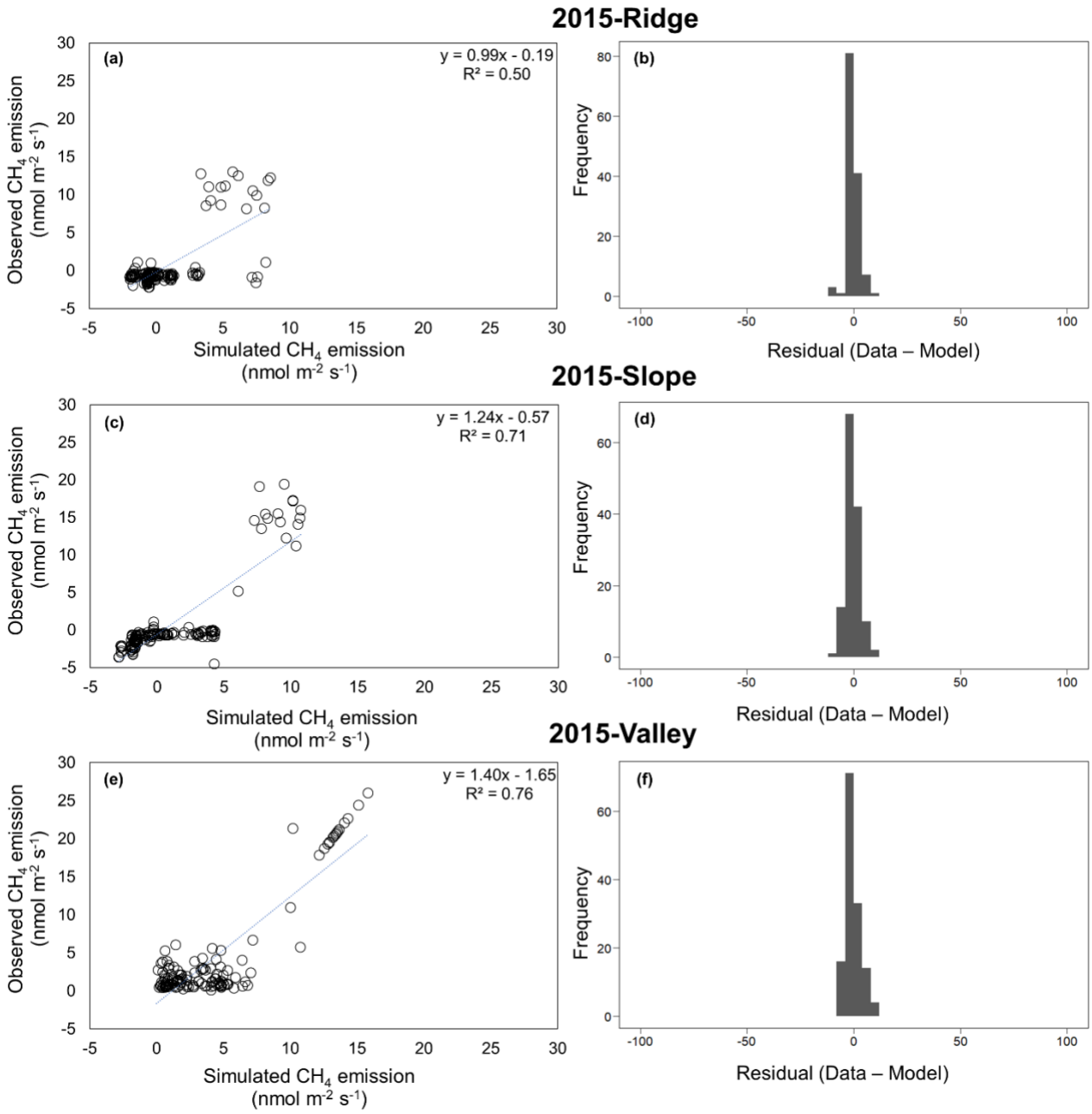

Figure S3: Observed versus simulated methane (CH_4) emission across landscape topography in 2015 in ridge (a, b), slope (c, d), and valley (e, f) topographic locations.

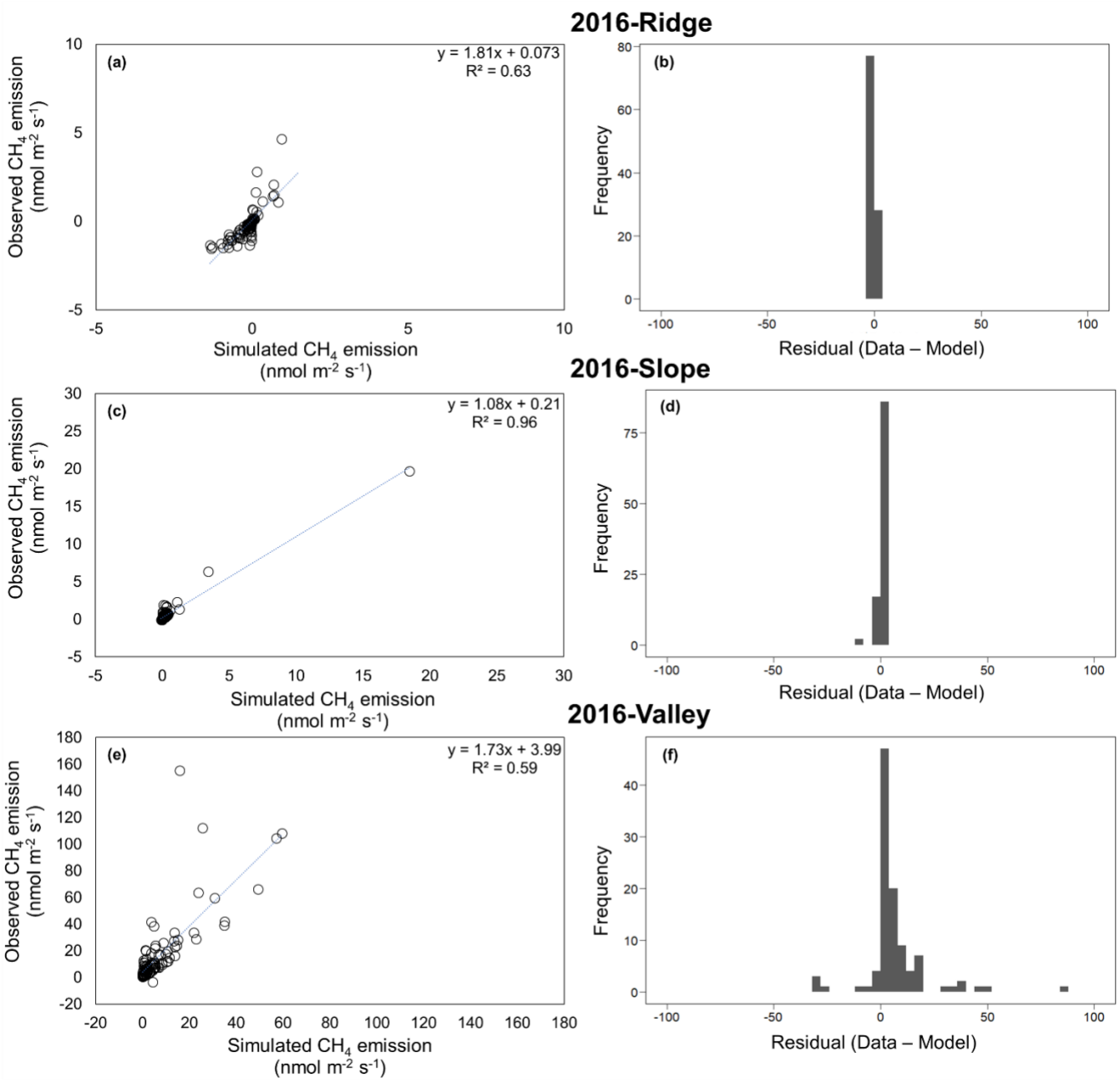

Figure S4: Observed versus simulated methane (CH_4) emission across landscape topography in 2016 in ridge (a, b), slope (c, d), and valley (e, f) topographic locations.

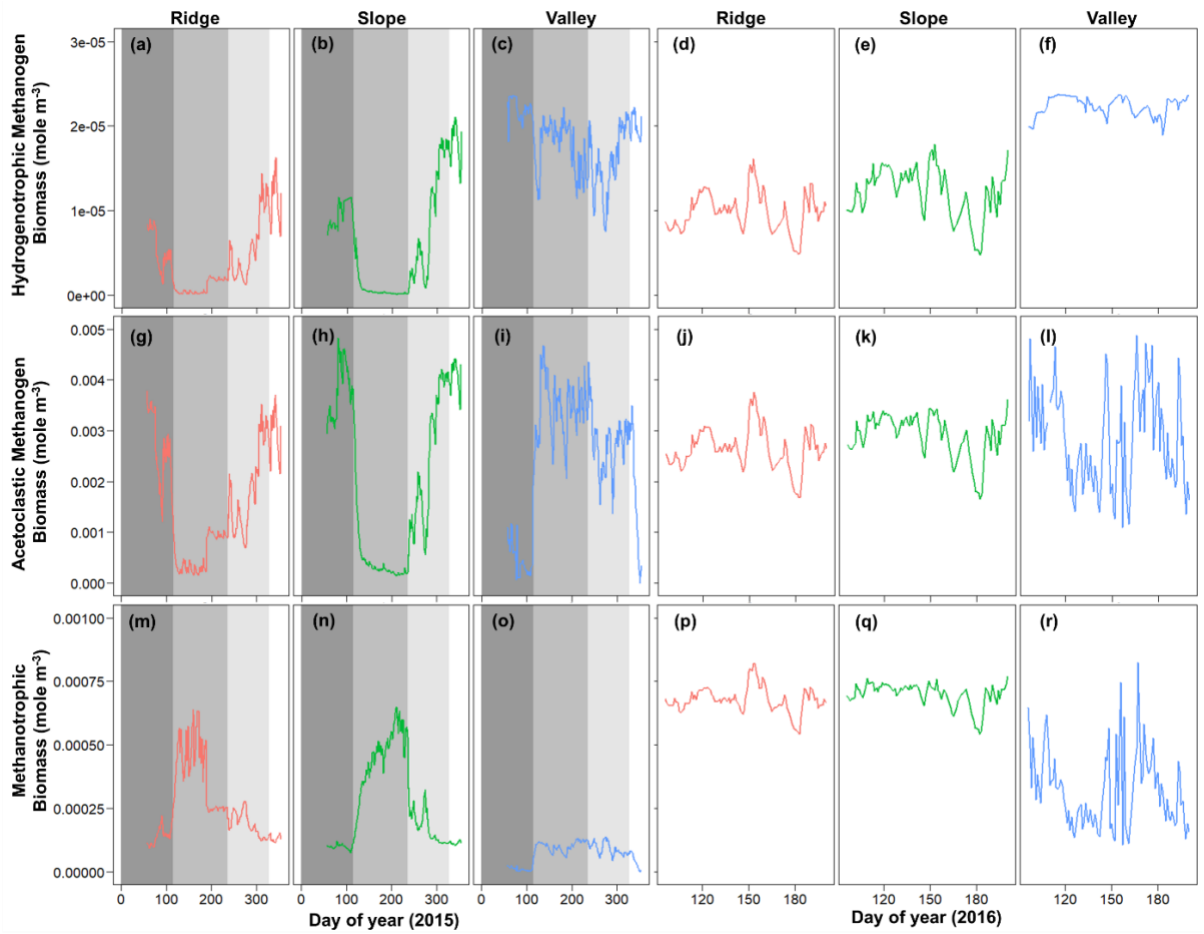

Figure S5: Temporal trend of microbial functional groups (hydrogenotrophic methanogens (a-f), acetoclastic methanogens (g-l), and methanotrophs (m-r)) across ridge-slope-valley topographic gradient. Dark gray, medium gray, light gray, and white shading represents pre-drought, drought, drought-recovery, and post-drought events in 2015 (O'Connell et al., 2018).

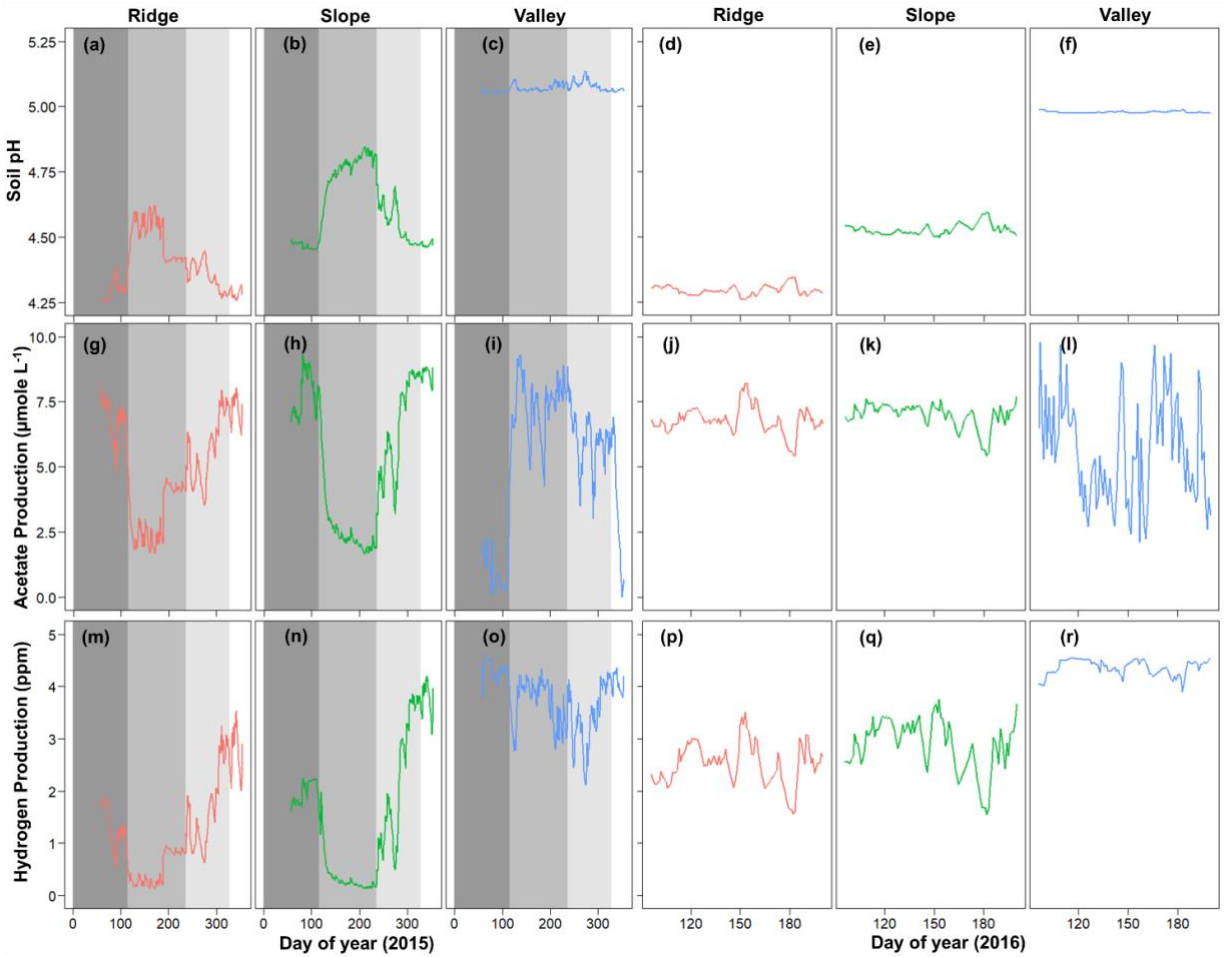

Figure S6: Temporal trend of soil pH (a-f), acetate production (g-l), and hydrogen production (m-r) across ridge-slope-valley topographic gradient. Dark gray, medium gray, light gray, and white shading represents pre-drought, drought, drought-recovery, and post-drought events in 2015 (O'Connell et al., 2018).

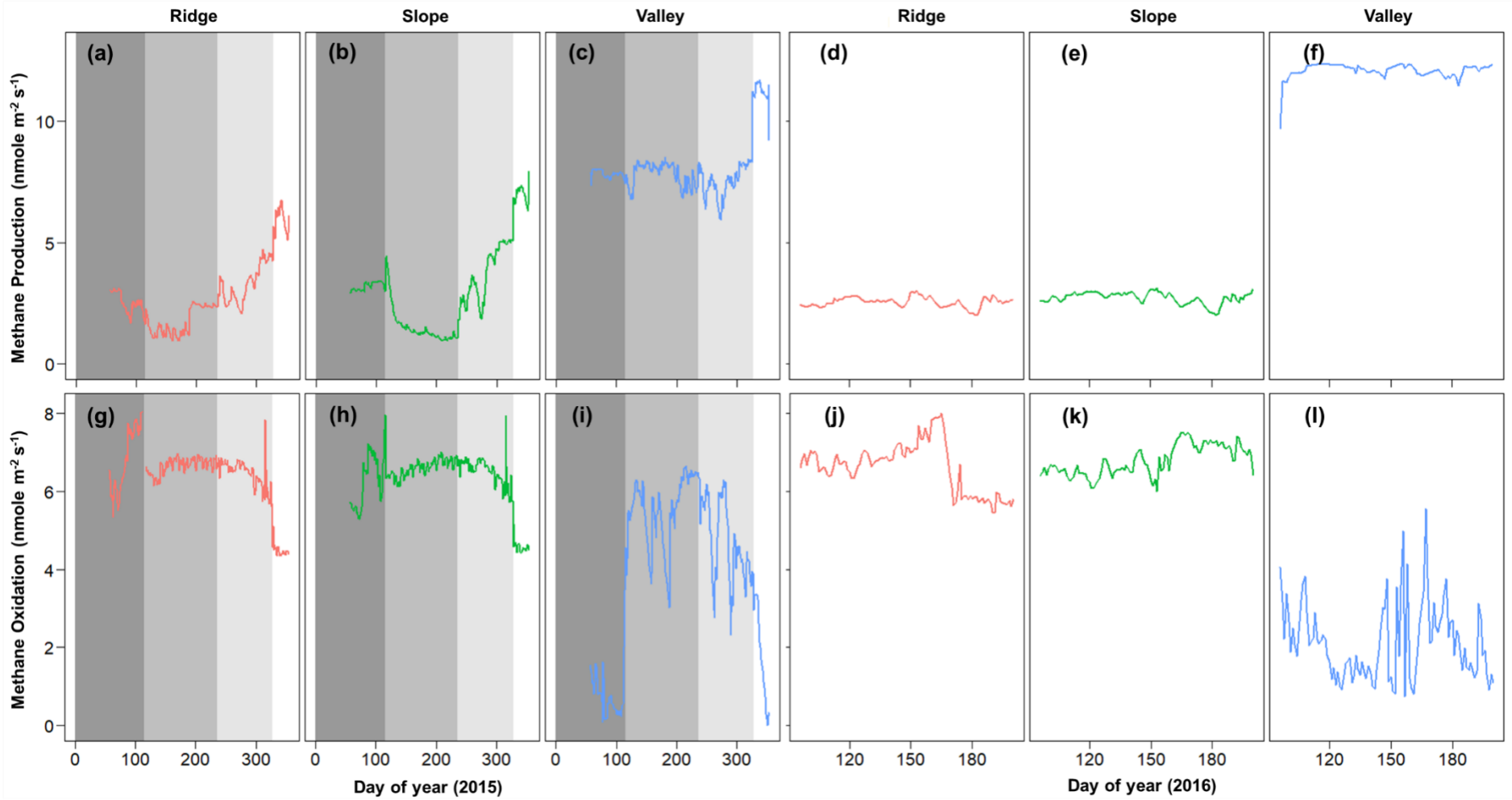

Figure S7: Temporal trend of gross methane (CH_4) production (a-f) and oxidation (g-l) across ridge-slope-valley topographic gradient. Dark gray, medium gray, light gray, and white shading represents pre-drought, drought, drought-recovery, and post-drought events in 2015 (O'Connell et al., 2018).

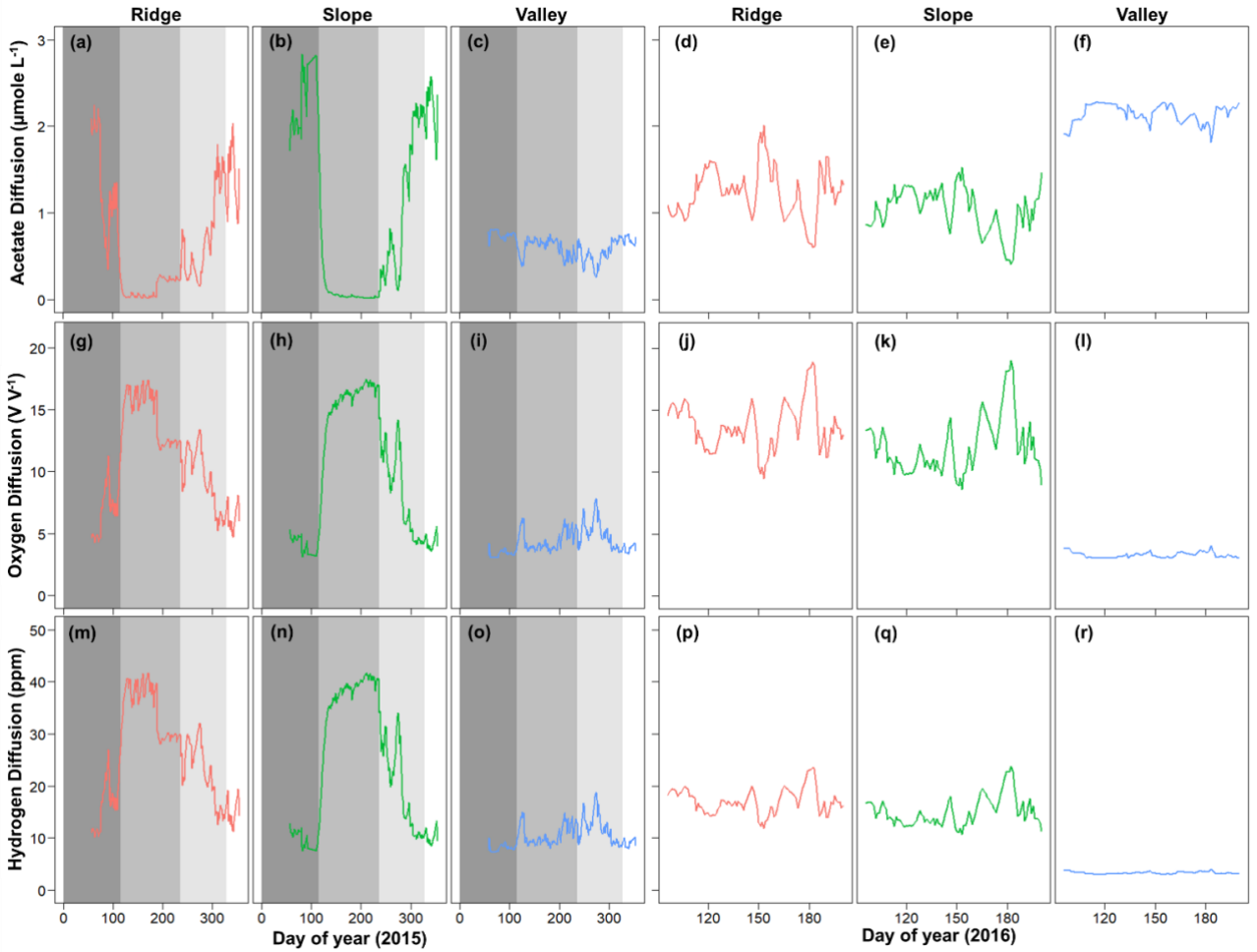

Figure S8: Temporal trend of acetate (a-f), oxygen (g-l), and hydrogen (m-r) delivery at microbial reaction site across ridge-slope-valley topographic gradient. Dark gray, medium gray, light gray, and white shading represents pre-drought, drought, drought-recovery, and post-drought events in 2015 (O'Connell et al., 2018).

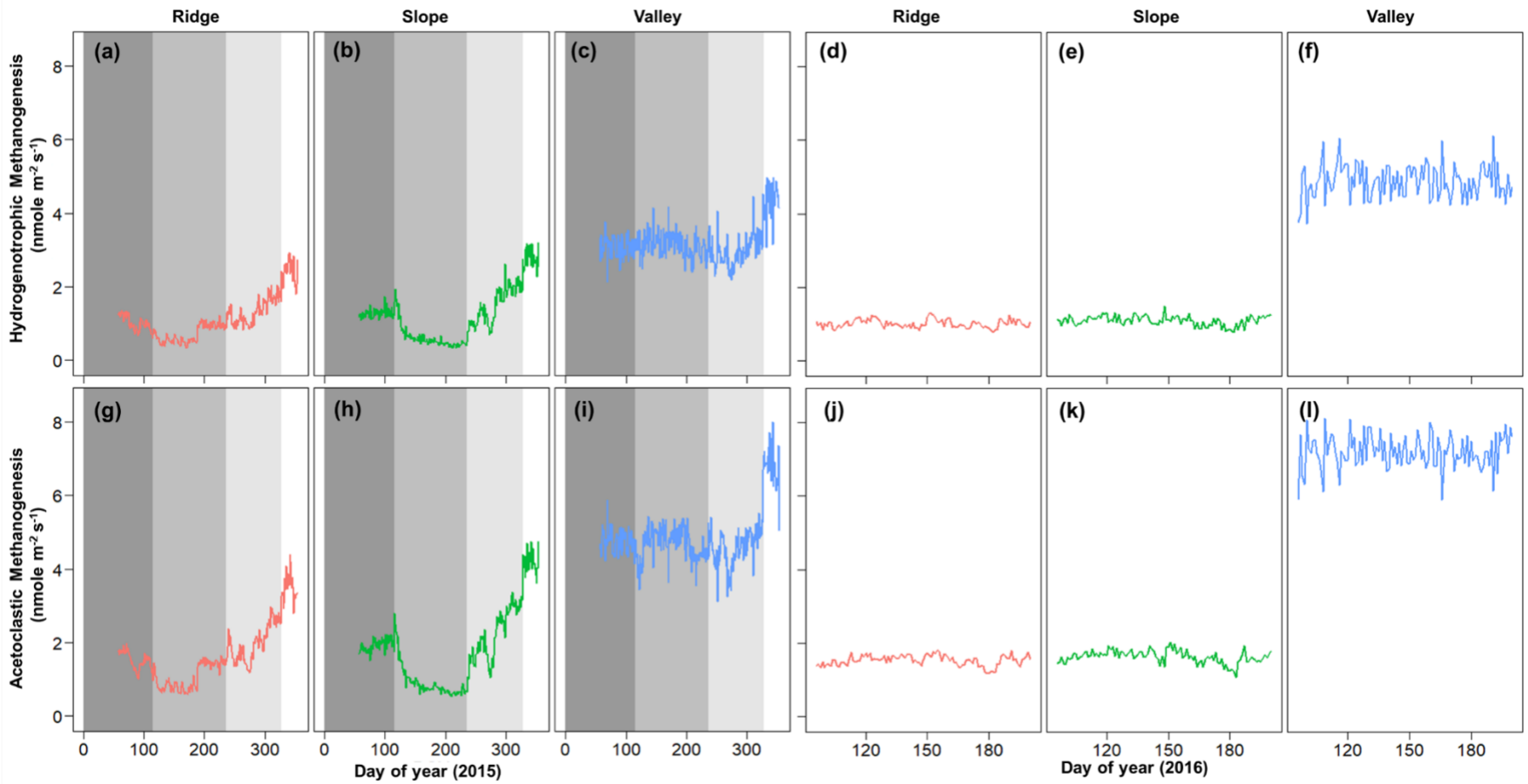

Figure S9: Temporal trend of hydrogenotrophic (a-f) and acetoclastic (g-l) pathways of methanogenesis across ridge-slope-valley topographic gradient. Dark gray, medium gray, light gray, and white shading represents pre-drought, drought, drought-recovery, and post-drought events in 2015 (O'Connell et al., 2018).

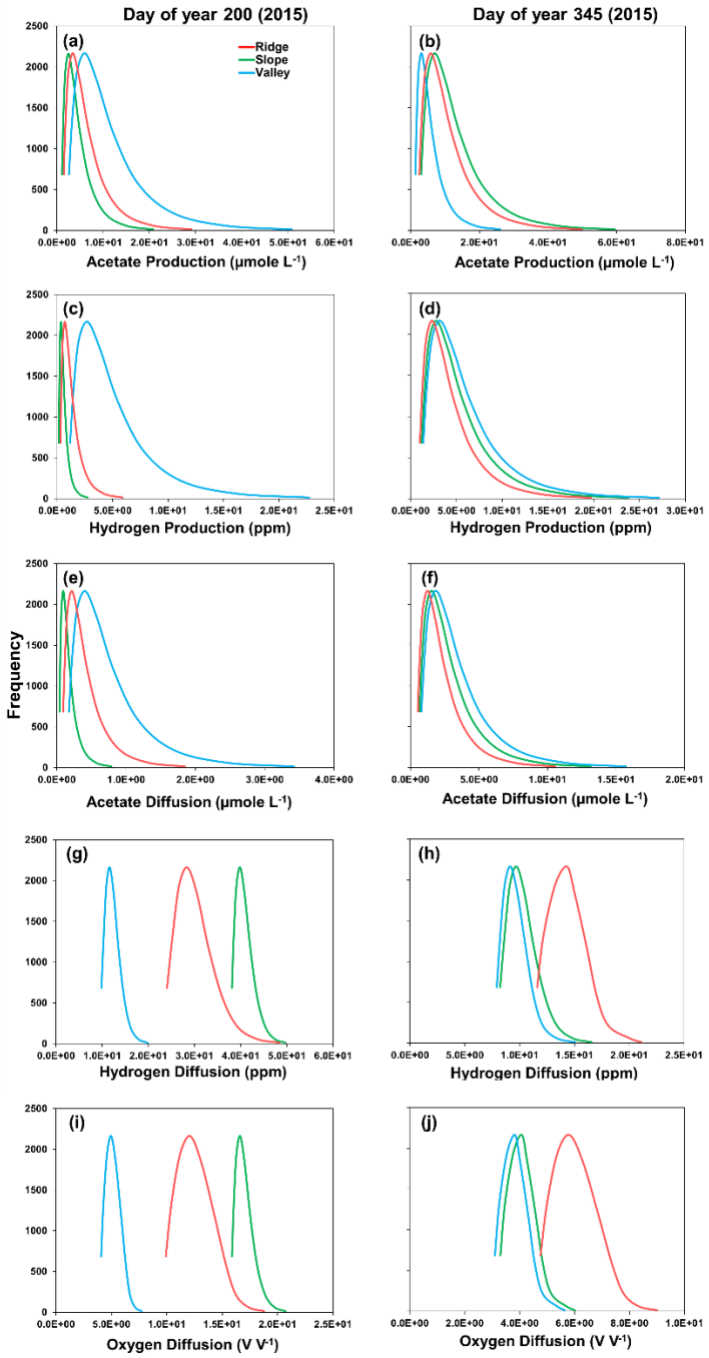

Figure S10: Rates of acetate production (a, b), hydrogen production (c, d), acetate diffusion (e, f), hydrogen diffusion (g, h), and oxygen diffusion (I, j) across simulated soil microsites. Day of year 200 and 345 represents drought and post-drought recovery events, respectively (see medium gray and white shading in Fig. 3).